How nanoparticles can induce dimerization and aggregation of cells in blood or lymph

BioSystems 210 (2021) 104551

Contents lists available at ScienceDirect

BioSystems

journal homepage: www.elsevier.com/locate/biosystems

Short communication

How nanoparticles can induce dimerization and aggregation of cells in blood or lymph

Vladimir P. Zhdanov *

Section of Nano and Biophysics, Department of Physics, Chalmers University of Technology, Göteborg, Sweden
Boreskov Institute of Catalysis, Russian Academy of Sciences, Novosibirsk, Russia

ARTICLE INFO

Keywords:
Nanoparticles
Cells
Vessels
Lipid membrane
Aggregation
Model

ABSTRACT

By analogy with virions, the binding of biologically-inspired nanoparticles (NPs) with ligands to the cellular membrane containing receptors depends on the multivalent ligand–receptor interaction, membrane bending, and cytoskeleton deformation. The interplay of these factors results in the existence of the potential minimum and activation barrier on the pathway towards full absorption of a NP. Herein, I hypothesize and show theoretically that the interaction of a NP, bound to one cell, with another cell can stabilize the potential minimum and increase the corresponding activation barrier, i.e., NPs can mediate the formation of long-living pairs of cells and aggregates containing a few cells inside blood and lymphatic vessels.

Nowadays, there are numerous efforts to use nanoparticles (NPs) in various biomedical applications (reviewed by Lane, 2020). In particular, there are attempts to employ biologically-inspired NPs for e.g. delivery of drugs and vaccines (reviewed by Mitchell et al., 2021) or virus targeting (reviewed by Jackman et al., 2020). In such applications, NPs are often expected to be transported along blood and lymphatic vessels. Although the corresponding chemical/biological physics has already been explored to some extent (reviewed by Lane, 2020; Zhdanov, 2021a; see also articles by Zhdanov, 2017a,b, 2019, 2021b, and references therein), this area is still in the formative stage and open for studies and discussions. The goal of this short Hypothesis Paper is to argue and articulate that such NPs can induce dimerization and aggregation of cells in blood or lymph and to clarify the underlying physics.

In applications, biologically-inspired NPs [e.g., lipid NPs (Mitchell et al., 2021)] are usually functionalized, and their size (~100 nm) and structure are often similar to those of enveloped virions, i.e., as already noticed in the abstract, their external protective layer contains ligands which can be bound with receptors located in the external membrane of cells. For this reason, the interaction of such NPs with the cellular membrane can be rationalized by analogy with that of virions (concerning virions, see e.g. models proposed by Sun and Wirtz, 2006; Zhdanov, 2013, 2015). In particular, the change of free energy during a contact of a NP with the cellular membrane [Fig. 1(a)] can be represented as a function of the engulfment depth (Zhdanov, 2017a)

$$\Delta F(h) = \Delta E_{\mathrm{lr}}(h) + \Delta E_{\mathrm{b}}(h) + \Delta E_{\mathrm{c}}(h), \tag{1}$$

where $\Delta E_{\mathrm{lr}} < 0$ is the ligand–receptor interaction, $\Delta E_{\mathrm{b}} > 0$ is the membrane bending energy, and $\Delta E_{\mathrm{c}} > 0$ is the deformation energy of the cytoskeleton or, more specifically, actin filaments. Roughly, ΔE_{lr} and ΔE_{b} are proportional to h. For spherically shaped NPs, for example, these contributions to the free energy are given by (Sun and Wirtz, 2006; Zhdanov, 2013)

$$\Delta E_{\mathrm{lr}}(h) \simeq -2\pi\alpha h R \quad \text{and} \quad \Delta E_{\mathrm{b}}(h) \simeq 4\pi\kappa h/R, \tag{2}$$

where R is the NP radius, α is the ligand–receptor interaction per unit area (or, in other words, a product of the ligand–receptor pair binding energy and 2D concentration of ligand–receptor pairs), and κ is the lipid-membrane bending rigidity. In practical situations, the ligand–receptor interaction is or can be designed to be sufficiently strong, so that ΔE_{lr} dominates. Thus, the sum of two terms in (2) can be expressed as

$$\Delta E_{\mathrm{lr}} + \Delta E_{\mathrm{b}} \simeq -Ah, \tag{3}$$

where $A = 2\pi\alpha R - 4\pi\kappa/R > 0$. The dependence of the cytoskeleton deformation energy on h is stronger and can roughly be represented as

$$\Delta E_{\mathrm{c}}(h) \simeq Bh^n, \tag{4}$$

where $B > 0$, and n is in the range from 2.5 to 4 depending on the specifics of the model (Sun and Wirtz, 2006; Zhdanov, 2013). This dependence is valid up to the critical value of the engulfment depth, $h \leq h_{\mathrm{cr}}$, and then ΔE_{c} drops with increasing h (Zhdanov, 2013). Below, this drop is implied but not described explicitly.

* Correspondence to: Boreskov Institute of Catalysis, Russian Academy of Sciences, Novosibirsk, Russia.
E-mail address: zhdanov@chalmers.se.

https://doi.org/10.1016/j.biosystems.2021.104551
Received 16 August 2021; Received in revised form 19 September 2021; Accepted 21 September 2021
Available online 29 September 2021

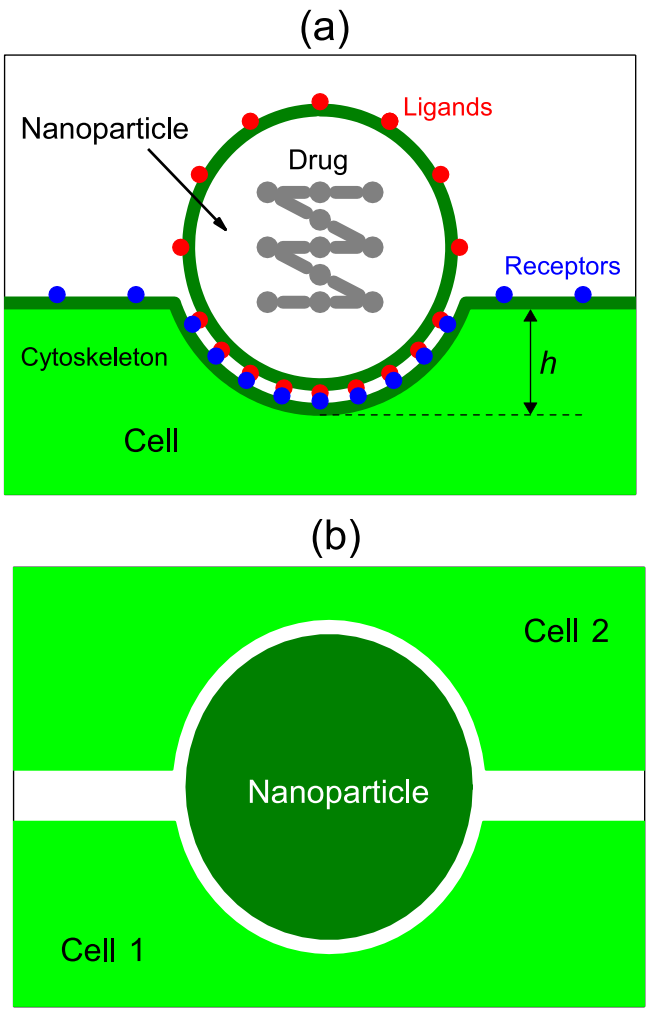

Fig. 1. Schemes of (a) engulfment of a NP into the host cell and (b) NP-mediated formation of a pair of cells. The NP structure [panel (a)] corresponds to biomedical applications.

Taken together, (3) and (4) allow one to rewrite (1) as

$$\Delta F(h) = -Ah + Bh^n. \tag{5}$$

With the specification above, this expression predicts the potential minimum at $h = h_* \equiv (A/nB)^{1/(n-1)}$ and activation barrier at $h = h_{cr} > h_*$ on the pathway towards full absorption of a NP.

In the terms of the model outlined, the optimization of the NP functionalization is a delicate process. The activation barrier for full absorption of NPs should not be too low, because otherwise NPs will be trapped just in the region of their injection and it may be not desirable. On the other hand, the barrier should not be too high, because otherwise NPs will be trapped just in the region of their injection as well if the barrier for detachment is high or the spatial distribution of NPs will be too wide if the barrier for detachment is low.

This situation is qualitatively similar to that with virions. In other words, this means that a NP is expected to attach to the membrane of a cell and to spend appreciable time before detachment or full absorption. If during this period, this cell contacts another cell and the attached NP is located in the contact region, it can interact with the latter cell as well and form a bridge between the two cells [Fig. 1(b)], i.e., the NP will mediate interaction between two cells so that they will form a long-living dimer. The corresponding change of free energy can be represented as a sum of the two terms describing the interaction on a

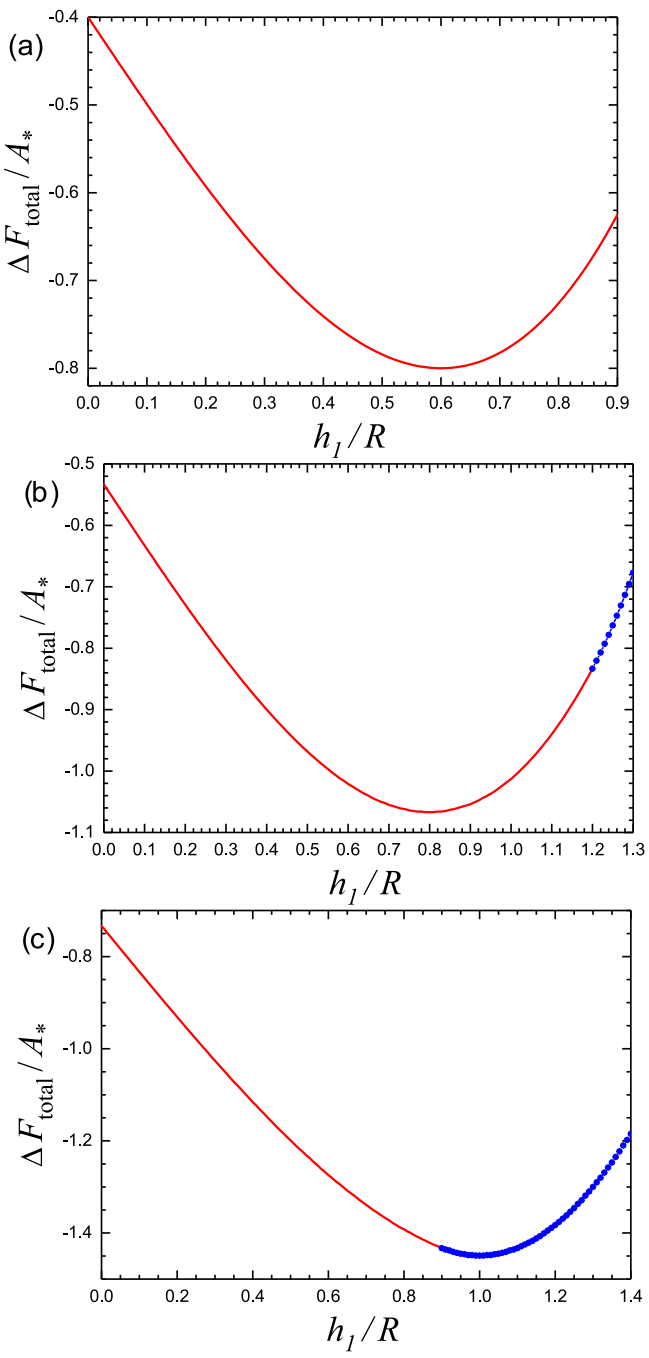

Fig. 2. Profiles of ΔF_{total} as a function of h_1/R at $0 \le h_1/R \le h_{cr}/R$ for (a) $h_*/R = 0.6$ and $h_{cr}/R = 0.9$, (b) $h_*/R = 0.8$ and $h_{cr}/R = 1.3$, and (c) $h_*/R = 1.1$ and $h_{cr}/R = 1.4$. In these examples, h_2/R is kept constant, $h_2/R = h_*/R$, provided this is compatible with a given value of h_1/R. If this is not the case, h_2/R is considered to be equal to $2 - h_1/R$. The former and latter are shown by solid lines and open circles, respectively.

NP with the cells and defined by (1),

$$\Delta F_{\text{total}}(h_1, h_2) = \Delta F(h_1) + \Delta F(h_2), \tag{6}$$

where h_1 and h_2 (with $h_1 + h_2 \le 2R$) are the NP engulfment depths for cells 1 and 2, respectively.

With the specification above, $\Delta F_{\text{total}}(h_1, h_2)$ given by (6) has a minimum either at $h_1 = h_2 = h_*$ (provided $h_* \le R$) or at $h_1 = h_2 = R$ (provided $h_* \ge R$). Depending on the relative values of these parameters and h_{cr} there are following three scenarios of the interaction of a NP with two cells, starting from the formation of a pair of cells with

$h_1 = h_2 = h_*$ or $h_1 = h_2 = R$ and its dissociation after the full absorption of a NP by one of the cells:

(i) If the ΔF_{total} minimum is at $h_1 = h_2 = h_* < R$ and $h_{\text{cr}} < 2R - h_*$, a NP plunged into one of the cells, e.g. cell 1, at $h_1 = h_*$ can plunge deeper from $h_1 = h_*$ to $h_1 = h_{\text{cr}}$ without perturbation of cell 2 which can be at equilibrium with $h_2 = h_*$. This process is energetically unfavourable as in the case of the endocytosis during the interaction of a NP with a single cell. Subsequent engulfment of a NP by cell 1 is energetically favourable, and at $h_1 > 2R - h_{\text{cr}}$ this can compensate the energy needed to decrease of the interaction with cell 2. Thus, the full engulfment will occur with the nearly same rate as in the case of a single cell. In particular, the potential barrier for the transition of a NP from equilibrium at $h_1 = h_*$ to full engulfment will be

$$\Delta U = \Delta F(h_{\text{cr}}) - \Delta F(h_*). \tag{7}$$

(ii) If the ΔF_{total} minimum is at $h_1 = h_2 = h_* < R$ and $h_{\text{cr}} > 2R - h_*$, a NP can plunge into one of the cells, e.g. cell 1, from $h_1 = h_*$ to $h_1 = h_{\text{cr}}$ only with perturbation of cell 2 which will in turn change h_2 from $h_2 = h_*$ to $2R - h_{\text{cr}}$. The latter costs energy, and the potential barrier for the transition of a NP from equilibrium at $h_1 = h_*$ to full engulfment will be higher than that given by (7). In particular, it will be given by

$$\Delta U = \Delta F(h_{\text{cr}}) + \Delta F(2R - h_{\text{cr}}) - 2\Delta F(h_*). \tag{8}$$

(iii) If $h_* \geq R$ and the ΔF_{total} minimum is at $h_1 = h_2 = R$, the corresponding value of ΔF_{total} is equal to $2\Delta F(R)$. At $h_1 = h_{\text{cr}}$ and $h_2 = 2R - h_{\text{cr}}$, the value of ΔF_{total} will be $\Delta F(h_{\text{cr}}) + \Delta F(2R - h_{\text{cr}})$. The potential barrier for the transition of a NP from equilibrium at $h_1 = h_*$ to full engulfment will accordingly be

$$\Delta U = \Delta F(h_{\text{cr}}) + \Delta F(2R - h_{\text{cr}}) - 2\Delta F(R). \tag{9}$$

To illustrate items (i)-(iii) more explicitly, it is instructive to normalize h by dividing by R and to rewrite (5) as

$$\Delta F(h) = -A_* \frac{h}{R} + B_* \left(\frac{h}{R}\right)^n, \tag{10}$$

where $A_* \equiv AR$ and $B_* \equiv BR^n$ are the constants with the dimension of energy. With these designations, the minimum of $\Delta F(h/R)$ is at $h/R = h_*/R \equiv (A_*/nB_*)^{1/(n-1)}$. For example, let us consider that $n = 3$. The typical profiles of $\Delta F_{\text{total}}(h_1, h_2)$ [Eq. (6)] calculated with this value of n are shown in Fig. 2 as a function of h_1/R. In these examples, the desirable value of h_*/R is determined by using the suitable value of A_*/B_*, whereas the value of h_{cr}/R was introduced axiomatically. h_2/R is kept constant, $h_2/R = h_*/R \equiv (A_*/nB_*)^{1/(n-1)}$, provided this is compatible with a given value of h_1/R. If this is not the case, h_2/R is considered to be equal to $2 - h_1/R$. In both cases, these prescriptions result in minimization of $\Delta F_{\text{total}}(h_1, h_2)$ at a given value of h_1/R.

The situation with $h_*/R = 0.6$ and $h_{\text{cr}}/R = 0.9$ [case (i)] is illustrated in Fig. 2(a) where the minimum of $\Delta F_{\text{total}}(h_1, h_2)$ is at $h_1/R = h_2/R = h_*/R = 0.6$, and reaching the activation barrier at $h_1/R = h_{\text{cr}}/R = 0.9$ is compatible with $h_2/R = h_*/R$. The situation with $h_*/R = 0.8$ and $h_{\text{cr}}/R = 1.3$ [case (ii)] is shown in Fig. 2(b) where the minimum of $\Delta F_{\text{total}}(h_1, h_2)$ is at $h_1/R = h_2/R = h_*/R = 0.8$, whereas reaching the activation barrier at $h_1/R = h_{\text{cr}}/R = 1.3$ is accompanied with the shift of h_2/R from 0.8 to 0.7. In the situation with $h_*/R = 1.1$ and $h_{\text{cr}}/R = 1.4$ [case (iii); Fig. 2(b)], the minimum of $\Delta F_{\text{total}}(h_1, h_2)$ is at $h_1/R = h_2/R = 1$, whereas reaching the activation barrier at $h_1/R = h_{\text{cr}}/R = 1.4$ is accompanied with the shift of h_2/R from 1 to 0.6.

Thus, the analysis above shows that NPs can induce the formation of dimers of cells. The formation of larger aggregates of cells is also possible. Concerning the stability of such dimers or aggregates, it is desirable to estimate the values of the potential barriers for dimer dissociation and for the full engulfment of a NP. The key parameters here are α, κ, B, and h_{cr}. The scale of α and κ is now known, whereas B and h_{cr} are related to the cytoskeleton deformation, and the corresponding accurate estimates are still difficult (Zhdanov, 2013). In the context of this communication, a more direct conclusion about the stability of dimers or aggregates can be drawn by (i) noticing that the corresponding potential barriers for NPs can be comparable with those for virions attached to the external membrane of cells and (ii) referring to experiments indicating that under such conditions virions can often be observed on the timescales from 1 min to 1 h (see, e.g., Ewers et al., 2005; Liu et al., 2020). This is indicative that by analogy with virions NPs can be long attached to the external membrane of cells, their interaction with the membrane can be appreciable, and they can induce the formation of dimers of cells. For viruses, the formation of such dimers does not appear to be favourable from the perspective of evolutionary biology, because it prevents penetration of virions into cell and their replication there. For this reason, the evolution of viruses was/is not expected to be in favour of inducing the formation of dimers or aggregates of cells. With this reservation, one can notice that, for example, influenza viruses are known to be able to bind to red blood cells and cause their clumping referred to as hemagglutination (Sánchez-Cano et al., 2021). Along this line, one can also notice e.g. that rotaviruses can induce fusion of cells (Falconer et al., 1995). The simplest mean-field kinetic model describing the formation of dimers at the population level was long proposed by Lanni and Lanni (1952). In the conventional kinetic models describing viral infection at this level, such processes are usually not taken into account (reviewed by Handel et al., 2020).

Thus, the above-formulated hypothesis that NPs can induce the formation of dimers of cells or larger aggregates is based on the robust physics, supported by the information available for viruses, and accordingly expected to be correct. If the latter is the case, the phenomenon predicted can be observed experimentally in academic studies and also *in vivo*. In academic studies, one can form a monolayer of cells at the floor of the chamber, expose these cells for a while to solution with NPs, and then to solution with other cells. By varying the number of ligands per NP, one can try to identify the conditions suitable for the formation of dimers of cells. *In vivo*, one can inject NPs, use the number of ligands per NP as a governing parameter as well, and then try to verify whether it results in the formation of dimers of cells or larger aggregates. The latter is of course not straightforward because the region/s where the dimerization and aggregation are most probable is/are not known in advance. Theoretically, the kinetics of the NP-induced aggregation of cells can be described by using the equations similar to those employed to interpret detection of biomolecules and biological NPs by means of induced aggregation of larger nanoparticles (Wahlsten et al., 2019). In the experiments aimed at detection, the concentrations of species are typically constant. During NP-mediated aggregation of cells *in vivo*, the concentration of NPs is expected to usually decrease due to their spreading. Thus, the latter problem is mathematically more complex.

Concerning potential biological implications of NP-induced formation of dimers of cells or larger aggregates for safety etc., the first expectation might be that this process is harmful. It may, however, be neutral or, perhaps, even positive under certain circumstances. This broad subject has now many uncertainties, and the related speculations are beyond my present goals. I may just notice that the aggregation of NPs is often briefly discussed in the context of safety of their use (reviewed, e.g., by Ganguly et al., 2018; Zhao et al., 2019). The NP-induced formation of dimers of cells or larger aggregates is, however, usually not mentioned there.

Declaration of competing interest

The author declares that he has no known competing finan-cial interests or personal relationships that could have appeared toinfluence the work reported in this paper.

Acknowledgement

This work was supported by Ministry of Science and Higher Education of the Russian Federation within the governmental order for Boreskov Institute of Catalysis (project AAAA-A21-121011390008-4).

References

Ewers, H., Smith, A.E., Sbalzarini, I.F., Lilie, H., Koumoutsakos, P., Helenius, A., 2005. Single-particle tracking of murine polyoma virus-like particles on live cells and artificial membranes. Proc. Natl. Acad. Sci. USA 102, 15110–15115.

Falconer, M.M., Gilbert, J.M., Roper, A.M., Greenberg, H.B., Gavora, J.S., 1995. Rotavirus-induced fusion from without in tissue culture cells. J. Virol. 69, 5582–5591.

Ganguly, P., Breen, A., Pillai, S.C., 2018. Toxicity of nanomaterials: exposure, pathways, assessment, and recent advances. ACS Biomat. Sci. Eng. 4, 2237–2275.

Handel, A., La Gruta, N.L., Thomas, P.G., 2020. Simulation modelling for immunologists. Nat. Rev. Immunol. 20, 186–195.

Jackman, J.A., et al., 2020. Biomimetic nanomaterial strategies for virus targeting: antiviral therapies and vaccines. Adv. Funct. Mater. 2008352.

Lane, L.A., 2020. Physics in nanomedicine: phenomena governing the *in vivo* performance of nanoparticles. Appl. Phys. Rev. 7, 011316.

Lanni, F., Lanni, Y.T., 1952. A quantitative theory of influennza virus hemagglutination-inhibition. J. Bacteriol. 64, 865–882.

Liu, S.-L., Wang, Z.-G., Xie, H.-Y., Liu, A.A., Lamb, D.C., Pang, D.-W., 2020. Single-virus tracking: from imaging methodologies to virological applications. Chem. Rev. 120, 1936–1979.

Mitchell, M.J., et al., 2021. Engineering precision nanoparticles for drug delivery. Nat. Rev. Drug. Discov. 20, 101–124.

Sánchez-Cano, A., Andrés, C., Herance, J.R., Pumarola, T., Antón, A., Baldrich, E., 2021. Detection of viruses and virus-neutralizing antibodies using synthetic erythrocytes: toward a tuneable tool for virus surveillance. ACS Sens. 6, 83–90.

Sun, S.X., Wirtz, D., 2006. Mechanics of enveloped virus entry into host cells. Biophys. J. 90, L10–L12.

Wahlsten, O., et al., 2019. Quantitative detection of biological nanoparticles in solution via their mediation of colocalization of fluorescent liposomes. Phys. Rev. Appl. 12, 064021.

Zhao, Z., Ukidve, A., Krishnan, V., Mitragotri, S., 2019. Effect of physicochemical and surface properties on *in vivo* fate of drug nanocarriers. Adv. Drug Deliv. Rev. 143, 3–21.

Zhdanov, V.P., 2013. Physical aspects of the initial phase of endocytosis. Phys. Rev. E 88, 064701.

Zhdanov, V.P., 2015. Kinetics of virus entry by endocytosis. Phys. Rev. E 91, 042715.

Zhdanov, V.P., 2017a. Multivalent ligand–receptor-mediated interaction of small filled vesicles with a cellular membrane. Phys. Rev. E 96, 012408.

Zhdanov, V.P., 2017b. Kinetics of lipid-nanoparticle-mediated intracellular mRNA delivery and function. Phys. Rev. E 96, 042406.

Zhdanov, V.P., 2019. Intracellular RNA delivery by lipid nanoparticles: diffusion, degradation, and release. BioSystems 185, 104032.

Zhdanov, V.P., 2021a. Virology from the perspective of theoretical colloid and interface science. Curr. Opin. Coll. Interf. Sci. 53, 101450.

Zhdanov, V.P., 2021b. Kinetic aspects of virus targeting by nanoparticles in vivo. J. Biol. Phys. 47, 95–101.